

Metal π complexes of benzene derivatives Part 56.[☆] (η^6 -Fluoranthene)(tricarbonyl)chromium: isomerism and haptotropic equilibration

Yuri Oprunenko ^{a,*}, Svetlana Malyugina ^a, Alexander Vasil'ko ^b,
Konstantine Lyssenko ^b, Christoph Elschenbroich ^{c,*}, Klaus Harms ^c

^a Department of Chemistry, M.V. Lomonosov Moscow State University, Vorob'evy Gory, 119899 Moscow, Russia

^b A. N. Nesmeyanov Institute of Organoelement Compounds, Russian Academy of Sciences, V-334 Vavilov Street 28, 117813 Moscow, Russia

^c Fachbereich Chemie der Philipps-Universität Marburg, Hans-Meerwein-Strasse, D-35032 Marburg, Germany

Received 31 August 2001; accepted 19 September 2001

Dedicated to Professor Rolf Gleiter on the occasion of his 65th birthday

Abstract

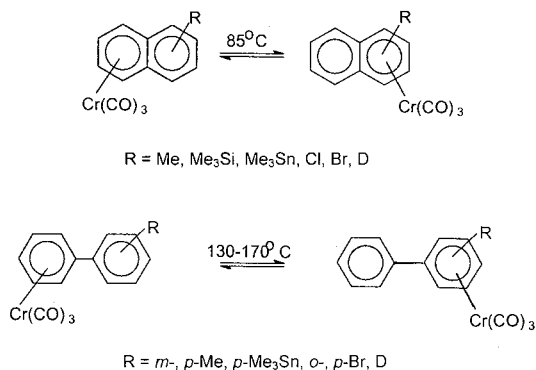
Reaction of fluoranthene with $\text{Cr}(\text{CO})_3\text{Py}_3/\text{BF}_3\cdot\text{OEt}_2$ at 25 °C affords a mixture of two isomeric complexes: traces of tricarbonyl(1-5,15- η^6 -fluoranthene)chromium (**3**) (coordination to benzene) and, as the major product, tricarbonyl(1-4,15,16- η^6 -fluoranthene)chromium (**2**) (coordination to naphthalene). The ratio **3:2** is less than 0.05 according to ¹H-NMR of crude product before crystallization. Complex **2** is thermodynamically less stable than **3**: at 100 °C in decane or C₆D₆ for 8 h or at 90 °C in C₆F₆ for 100 h **2** rearranges irreversibly to **3** via an inter-ring haptotropic shift of the Cr(CO)₃ group from the naphthalene moiety to the benzene part of the fluoranthene ligand. NMR evidence for a degenerate reversible haptotropic shift within the naphthalene moiety is absent. The isomers **2** and **3** have been characterized by X-ray structural analysis. © 2002 Elsevier Science B.V. All rights reserved.

Keywords: Fluoranthene; Tricarbonyl chromium complexes; Haptotropic rearrangements; X-ray structural analysis; ¹H- and ¹³C-NMR

1. Introduction

π -Complexes of transition metals with polycyclic aromatic hydrocarbons (PAH), in which only a part of the ligand perimeter accessible for coordination is involved in bonding to a metal atom, typically display high lability. Among the dynamic processes that may occur in these compounds are intramolecular inter-ring haptotropic rearrangements (IHR), which entail migration of an L_nM fragment from one position of the ligand to another. This type of thermally induced rearrangement was observed previously for various tricarbonyl chromium complexes with PAH ligands [1,2], in partic-

ular with naphthalene [3–5] and biphenyl [6,7] derivatives (Scheme 1). In such complexes the Cr(CO)₃ fragment in inert, non-coordinating solvents like decane or C₆F₆ at 80–170 °C intramolecularly shifts between substituted and unsubstituted rings of the ligand with

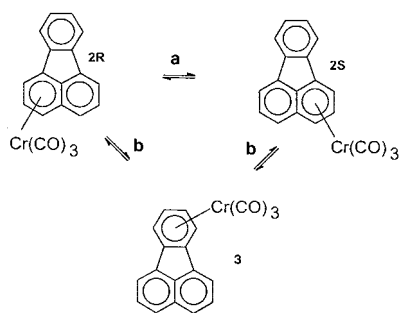


[☆] For Part 55, see Organometallics 20 (2001) 1875.

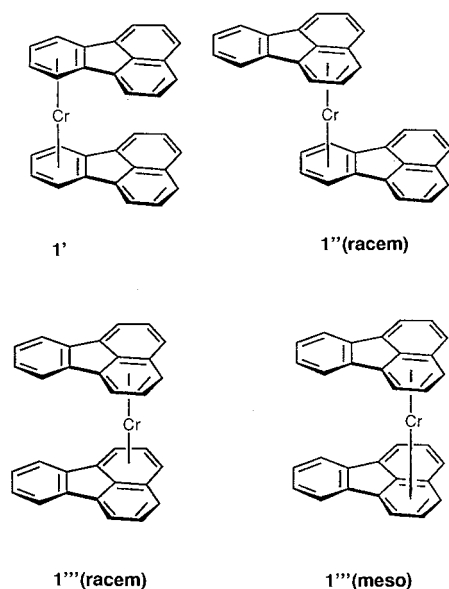
* Corresponding author. Tel.: +49-6421-282-5527; fax: +49-6421-282-5653.

E-mail address: eb@chemie.uni-marburg.de (C. Elschenbroich).

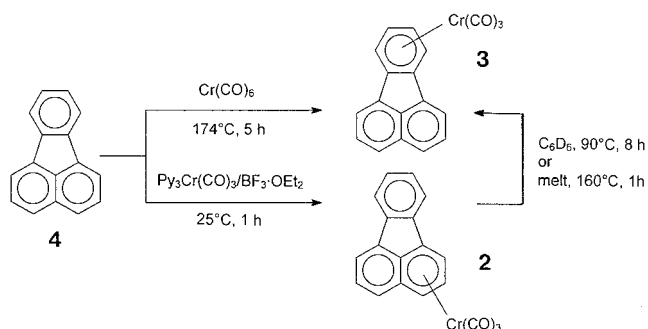
Scheme 1.



Scheme 2.



Scheme 3.



Scheme 4.

an activation barrier of 27–33 kcal mol⁻¹ (η^6, η^6 -rearrangements) [4,8]. These processes have been monitored by methods of stationary kinetics (e.g. HPLC and NMR) [8,9]. A theoretical analysis of haptotropic shifts has been given by Albright et al. [10]. Yet, to our knowledge, all attempts to detect degenerate η^6, η^6 -haptotropic shifts in transition metal complexes of naphthalene ligands devoid of a substituent label at one of the six-membered rings by means of dynamic NMR

have failed. On heating, the ¹H- and ¹³C-NMR spectra of (η^6 -naphthalene)Cr(CO)₃, 110 °C, Bu₂O or sulfolane [11] or 140 °C, decane [12]; [(η^6 -naphthalene)Ir(C₅Me₅)](PF₆)₂, 70 °C, CF₃COOH [13]; (η^6 -acenaphthylene)CrCO₃ [10] and (η^6 -naphthalene)₂Cr, 130 °C, C₆D₆ [14] did not change. Degenerate η^2, η^2 -haptotropic shifts have, however, been observed for L₂Ni complexes of naphthalene [15] and anthracene [16] (L = organophosphane ligand), they were studied in the solid state by means of CP MAS NMR techniques [15] and in fluid solution via spin saturation transfer experiments [16]. Shifts between C=C double bonds of one as well as of two different rings of the respective PAH could thereby be detected.

An interesting situation arises with fluorene since this ligand features a benzene and a naphthalene moiety which are *peri*-condensed. Obviously, a transition metal fragment η^6 -coordinated to one of the three possible coordination sites has the option of either engaging in an IHR within the naphthalene unit (type **a**, Scheme 2) or of a shift between the rings of the naphthalene and the benzene sections of the ligand (type **b**, Scheme 2). Whereas **a** would represent a degenerate rearrangement, **b** should lead to an equilibrium mixture of two isomers, reflecting the differing thermodynamic stabilities of the components. By means of metal-atom ligand-vapor co-condensation techniques we have recently prepared the sandwich complex bis(η^6 -fluorene)chromium **1** and reported on the isomer distribution (Scheme 3) as affected by work-up conditions and thermal treatment [17]. Clearly, isomer **1'**, in which chromium binds to the benzene moiety of fluorene, is thermodynamically favored. In this communication we extend these studies to half-sandwich complexes of the (η^6 -arene)Cr(CO)₃ type, posing the question whether the processes **a** and **b** can be observed separately and which of the isomers represents the species of maximum stability. The study also aimed at the characterization of both isomers by means of X-ray diffraction.

2. Results and discussion

In order to explore the dependence of product composition on temperature we prepared (η^6 -fluorene)(tricarbonyl)chromium by two methods, namely the original high-temperature (ht) method of Fischer and coworkers, starting from Cr(CO)₆ [18], and by the low temperature (lt) process developed by Öfele, employing (pyridine)₃Cr(CO)₃ in the presence of BF₃·OEt₂ [19] (Scheme 4). Whereas ht substitution affords pure **3** as dark red crystals, lt substitution leads to a mixture of three isomers in which **2** (*R,S*) dominates and **3** is present in a relative yield of $\leq 5\%$. After recrystallization from benzene–heptane, pure **2** is ob-

tained as violet crystals. Accordingly, **2** represents the kinetically controlled and **3** the thermodynamically controlled product. In previous work [18] only the latter had been obtained. The coordination modes in **2** and **3** follow from the ^1H - and ^{13}C -NMR spectra. Assignments of ^1H -NMR signals are based on double resonance and Overhauser effect measurement, using the NOE DIF technique. ^{13}C -NMR signals were assigned by means of DEPT and through comparison with the data of related compounds. In both cases, the typical high-field coordination shifts and the coordination induced decrease in scalar $^1\text{H}, ^1\text{H}$ couplings proved helpful.

Since structural information on pairs of isomeric (PAH) $\text{Cr}(\text{CO})_3$ complexes is rare we have subjected the compounds **2** and **3** to single crystal X-ray diffraction. The molecular structures of **2** and **3** are depicted in Figs.

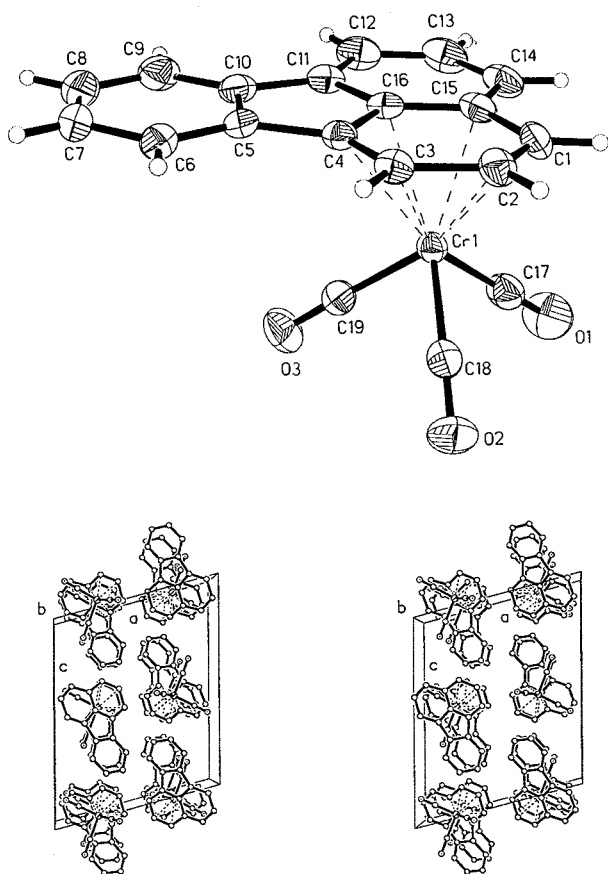


Fig. 1. Molecular structure of compound **2**, SHELXTL-PLUS drawing with 50% probability ellipsoids and numbering scheme. Selected bond lengths (pm): C1–C2, 139.8(3); C2–C3, 143.0(3); C3–C4, 140.0(3); C4–C16, 142.3(3); C11–C16, 142.2(3); C11–C12, 136.9(3); C12–C13, 142.8(4); C13–C14, 136.4(3); C14–C15, 142.4(3); C15–C1, 143.9(3); C15–C16, 140.7(3); C4–C5, 147.6(3); C10–C11, 147.4(3); C5–C6, 138.1(3); C6–C7, 139.6(3); C7–C8, 138.8(4); C8–C9, 138.1(4); C9–C10, 138.9(3); C10–C5, 142.1(3); Cr–C1, 222.1(2); Cr–C2, 220.4(2); Cr–C3, 222.5(2); Cr–C4, 224.0(2); Cr–C16, 227.2(2); Cr–C15, 230.6(2); Cr–C17, 185.0(2); Cr–C18, 182.8(2); Cr–C19, 183.8(2).

1 and **2**, respectively, and the important bond lengths are given in the captions. In their structural features the two isomers **2** and **3** to a large extent resemble those of the respective parent complexes (η^6 -benzene)(tricarbonyl)chromium [20] and (η^6 -naphthalene)(tricarbonyl)chromium [21]. Thus, in **2** and **3** the η^6 -arene and $\text{Cr}(\text{CO})_3$ moieties assume a staggered conformation. Ring slippage is minute in both cases, the displacement of the projection of the chromium atom from the ring centroid toward the ligand periphery, away from the annelated section of the ring, amounting to 6.7 pm (**2**) and 3.5 pm (**3**) only. This movement represents a shift of the central metal toward the region of higher intra-ligand π -bond order; interestingly, this direction is opposite to the path [10] the $\text{Cr}(\text{CO})_3$ fragment is thought to travel during the IHR process which we will now examine.

Fluoranthene **4** contains a naphthalene as well as a biphenyl unit both of which may form the scaffold for haptotropic shifts. Therefore, in (η^6 -fluoranthene) $\text{Cr}(\text{CO})_3$ the possibilities of either degenerate intra-naphthalene or non-degenerate intra-biphenyl shifts of the $\text{Cr}(\text{CO})_3$ fragment exist. Heating a melt of **2** to 160 °C for 1 h yields pure **3** (Scheme 4). Similarly, heating a solution of **2** in decane to 90–100 °C (preparative scale) or in C_6D_6 or C_6F_6 to 80–90 °C (^1H -NMR tube) leads to gradual disappearance of **2** and the formation of **3**. This rearrangement was monitored by chromatography and by ^1H -NMR either after removal of decane or directly in solution. After 8 h at 100 °C both in decane and in C_6D_6 , **2** fully rearranged to **3**. Interestingly, this type **b** haptotropic shift proceeds under somewhat milder thermal conditions than that depicted in Scheme 1. Conceivably, the planar structure of the biphenyl moiety in **2** and **3**, as opposed to the twisted structure in the η^6 -biphenyl complexes of Scheme 1, is responsible for the acceleration. Neither by TLC nor by ^1H -NMR did we observe any decomposition of the complexes **2** and **3** during IHR under the above-mentioned conditions, no free ligand or complex $\text{C}_6\text{D}_6\text{Cr}(\text{CO})_3$ being detected as a result of an exchange reaction in C_6D_6 . Such reactions are quite common for the derivatives of tricarbonyl(η^6 -naphthalene)chromium at temperatures above 140 °C [12]. Accordingly, for the complex **2** ligand displacement of fluoranthene by C_6D_6 sets in only at $T = 130$ °C, leading to the ratio $2:(\eta^6\text{-C}_6\text{D}_6)\text{Cr}(\text{CO})_3 = 1:1$ after 10 h and to complete ligand exchange after 30 h. After this time interval ^1H -NMR revealed the exclusive presence of non-coordinated ligand **4** and ^2D NMR attested to the formation of ($\eta^6\text{-C}_6\text{D}_6$) $\text{Cr}(\text{CO})_3$. Finally, heating of pure **3** both in solution (decane, C_6D_6) or as a melt fails to afford **2** thereby pointing to the irreversible nature of the IHR process **2** \rightarrow **3**.

In order to provide a more quantitative description, the rate for the conversion **2** \rightarrow **3** was determined taking

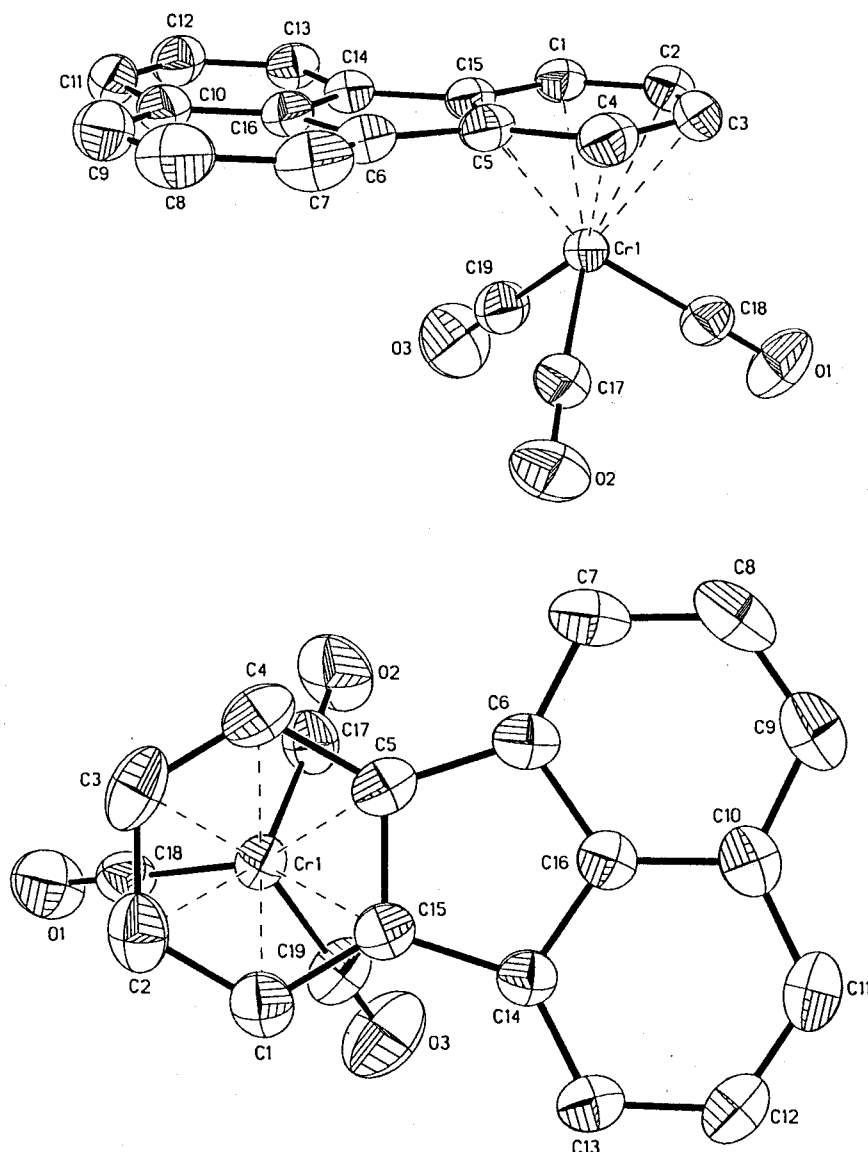


Fig. 2. Molecular structure of compound **3**, SHELXTL/XP drawing with 50% probability ellipsoids and numbering scheme. Selected bond lengths (pm): C1–C2, 138.9(3); C2–C3, 141.6(4); C3–C4, 139.2(4); C4–C5, 141.6(3); C5–C15, 142.6(3); C1–C15, 140.8(3); C5–C6, 147.1(3); C6–C7, 137.1(3); C7–C8, 141.4(4); C8–C9, 136.2(4); C9–C10, 142.0(3); C10–C11, 141.3(3); C11–C12, 136.6(3); C12–C13, 141.4(3); C13–C14, 136.8(3); C14–C16, 140.7(3); C14–C15, 147.1(3); C10–C16, 139.6(3); Cr–C1, 223.5(2); Cr–C2, 220.3(2); Cr–C3, 220.9(2); Cr–C4, 223.1(2); Cr–C5, 225.9(2); Cr–C15, 224.3(2); Cr–C17, 183.3(2); Cr–C18, 184.1(2); Cr–C19, 183.8(2).

advantage of the distinctive $^1\text{H-NMR}$ spectra of the participants. Kinetic curves documenting the change in solution composition during the isomerization are shown in Fig. 3a, a plot of $\ln(2_0/2_t)$ versus time, which should be linear for an irreversible first-order reaction, is presented in Fig. 3b. Consideration of data collected after longer reaction times does not add to precision since decomposition via metal ligand cleavage, possibly an autocatalytic process, becomes detectable after 40 h at 90 °C in C_6F_6 , amounting to approximately 10% cleavage after 130 h. After 230 h, conversion of **2** to **3** is practically complete, at this time $\approx 60\%$ metal–ligand cleavage has occurred, however. From the data

recorded for the initial reaction period of 70 h, where decomposition is marginal, and based on the rate law for a first order reaction $2 \rightarrow 3$, $kt = \ln(2_0/2_t)$, the rate constant $k_{90} = (6.82 \pm 0.16)10^{-6} \text{ s}^{-1}$ is obtained. The free energy of activation calculated by means of the relation $\Delta G_{\ddagger}^\ddagger = 4.576 (10.319 + \lg T - \lg k_T)$ amounts to $\Delta G_{363}^\ddagger = 32.6 \text{ kcal mol}^{-1}$.

In principle, IHR in **2** constitutes a three-site problem since a $\text{Cr}(\text{CO})_3$ fragment, bonded to one of the six-membered rings of the naphthalene moiety, has the options to migrate either to the second C_6 unit within naphthalene or to the anellated benzene ring. However, within the temperature range covered in the present

investigation, NMR evidence for a degenerate haptotropic shift within the naphthalene moiety of the fluoranthene ligand is absent. Apparently, the higher driving force/lower activation energy shift to the anellated benzene ring dominates and the $\text{Cr}(\text{CO})_3$ fragment is trapped in the latter. This course gains plausibility from a consideration of the results of quantum chemical studies dealing with the path, the $\text{Cr}(\text{CO})_3$ unit follows in η^6, η^6 -haptotropic rearrangements of naphthalenechromium tricarbonyl [10]. Herein it was shown that the shortest path across the central C–C bond is forbidden and, instead, a path is preferred in which the $\text{Cr}(\text{CO})_3$ unit moves towards the periphery of the naphthalene ligand. Therefore, the approaches toward the transition state for the two alternative shifts (η^6 -naphthalene \rightarrow η^6 -naphthalene vs. η^6 -naphthalene \rightarrow η^6 -benzene) may bear some similarity. To the extent that the transition state is product-like, the shift to the anellated benzene ring will then be preferred since it leads to the thermodynamically favored complex **3**.

3. Experimental

3.1. General

All operations were performed under a purified argon atmosphere. Ether was purified by refluxing over a K–Na alloy and distilled from it under argon prior to use. Decane was freed from water and oxygen by

storing on potassium mirror, further distillation and repeated freeze–pump–thaw cycles. If not specified, chromatography was carried out on silica 40/100 μ Chemapol (Bratislava, Slovak Republic). NMR spectra were recorded in a spectrometer Varian VXR-400 (400 MHz for ^1H). IR spectra were recorded in heptane on a UR-20 Carl Zeiss spectrometer. Mass spectra were measured in a Varian-CH7A instrument under an electron impact of 70 eV.

3.2. Synthesis of **2**

Freshly distilled $\text{BF}_3 \cdot \text{OEt}_2$ (5.20 g, 36.55 mmol) was added to a mixture of fluoranthene (1.60 g, 7.92 mmol) and $\text{Cr}(\text{CO})_3\text{Py}_3$ (3.0 g, 8.03 mmol) in 50 ml of ether at -10°C . After stirring at 25°C for 1 h water was added. The solution was washed three times with water and dried over anhydrous MgSO_4 . After the ether was removed in vacuo the residue was chromatographed on a 3×40 cm silica gel column using a petroleum ether–benzene mixture as eluent. From the violet zone 1.55 g (58%) of **2** was obtained after recrystallization from benzene–heptane. Complex **2** was crystallized from heptane as violet needles, m.p. 154 – 157°C . $^1\text{H-NMR}$ (300 K, C_6D_6 , 400.1 MHz, ppm): $\delta = 4.67$ (1H, t, $J_{\text{H8}/\text{H9}} = J_{\text{H8}/\text{H7}} = 6.40$ Hz, H8), 5.29 (1H, dd, $J_{\text{H7}/\text{H9}} = 0.58$ Hz, H7), 5.47 (1H, dd, H9), 7.57 (1H, m, H1), 7.30 (1H, m, H4), 7.13–7.16 (2H, m, H2, H3), 7.02 (2H, m, H12, H13), 7.19 (1H, dd, $J_{\text{H11}/\text{H12}} = 7.80$ Hz, $J_{\text{H11}/\text{H13}} = 0.8$ Hz, H11). $^1\text{H-NMR}$ (300 K, C_6F_6 , 400.1 MHz, ppm): $\delta = 5.72$ (1H, dd, $J_{\text{H8}/\text{H9}} = 6.80$ Hz, $J_{\text{H8}/\text{H7}} = 5.80$ Hz, H8), 6.39 (1H, dd, $J_{\text{H7}/\text{H9}} = 0.60$, H7), 5.47 (1H, dd, H9), 8.11 (1H, m, H1), 7.95 (1H, m, H4), 7.63–7.66 (2H, m, H2, H3), 7.86 (2H, m, H12, H13), 7.19 (1H, m, H11). $^{13}\text{C-NMR}$ (300 K, C_6D_6 100.6 MHz, ppm): $\delta = 87.57$ (C9), 87.18 (C7), 90.45 (C8), 101.60 (C10), 102.95 (C16), 106.00 (C6), 119.56, 122.06 (C1, C4), 122.55 (C13), 125.33 (C11), 128.49, 128.77 (C2, C3), 130.12 (C12), 137.41 (C14), 137.94, 139.43 (C5, C15), 231.78 (C0). Mass spectra: m/e 338 (3.1) [M^+]; 282 (6.6) [$\text{M} - 2\text{CO}^+$]; 254 (34.6) [$\text{M} - 3\text{CO}^+$]; 202 (100) [$\text{C}_{16}\text{H}_{10}^+$], 52 (67.8) [Cr^+]. ^1H - and ^{13}C -NMR data are presented in Table 1. IR (cm^{-1}): $\nu_{\text{CO}} = 1915, 1932, 1985$. $\text{C}_{19}\text{H}_{10}\text{O}_3\text{Cr}$: Calc.: C, 67.46; H, 2.96. Found: C, 66.83; H, 2.85%. Crystals suitable for X-ray diffraction were obtained by layering of solution of **2** (20 mg in 8 ml of benzene) with 40 ml of hexane at 5°C for ca. 2 weeks.

3.3. X-ray structure analysis of **2**

Accurate cell parameters and orientation matrices were obtained by least-squares refinement of 5000 peaks in the $2^\circ \leq 2\theta \leq 50^\circ$ range. The structure was solved by direct methods and subsequent difference Fourier maps. All hydrogen atoms were located in the

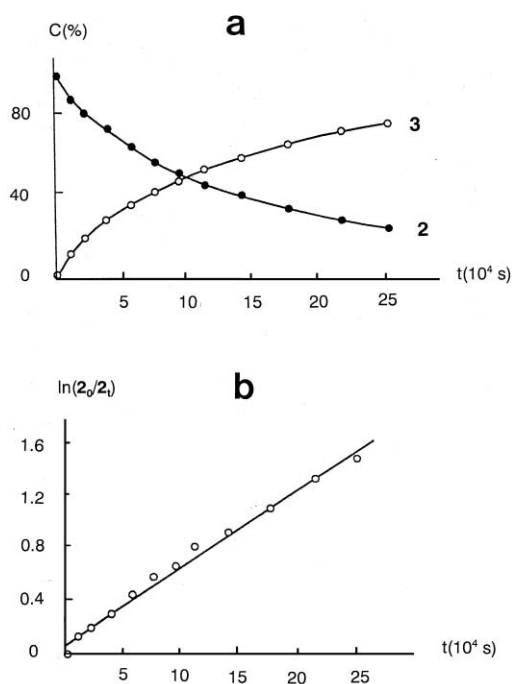


Fig. 3. (a) Kinetic curves for the thermal isomerization **2** \rightarrow **3** (IHR) in C_6F_6 at 90°C . (b) Kinetic first-order dependence for the irreversible thermal isomerization **2** \rightarrow **3** (IHR) in C_6F_6 at 90°C .

Table 1
Crystal data and structure refinement parameters for compounds **2** and **3**

	2	3
Empirical formula	C ₁₉ H ₁₀ CrO ₃	C ₁₉ H ₁₀ CrO ₃
Formula weight	338.27	338.27
Temperature (K)	193	293
Wavelength Mo–K _α (Å)	0.71073	0.71073
Crystal system	Monoclinic	Orthorhombic
Space group	<i>P</i> 2 ₁ / <i>c</i>	<i>Pbca</i>
Unit cell dimensions		
<i>a</i> (Å)	12.647(1)	13.367(4)
<i>b</i> (Å)	7.778(1)	13.131(3)
<i>c</i> (Å)	15.474(2)	16.572(4)
β (°)	105.094(12)	
<i>V</i> (Å ³)	1469.7(2)	2908.7(13)
<i>Z</i>	4	8
<i>D</i> _{calc} (g cm ⁻³)	1.529	1.545
Absorption coefficient μ(Mo–K _α) (cm ⁻¹)	7.90	7.98
<i>F</i> (000)	688	1376
Crystal size (mm)	0.23 × 0.18 × 0.04	0.4 × 0.4 × 0.6
Diffractometer used	Stoe IPDS	Siemens P3
Theta range (°)	2.80–25.93	2.46–25.05
Index ranges	–15 ≤ <i>h</i> ≤ 15, –9 ≤ <i>k</i> ≤ 8, –18 ≤ <i>l</i> ≤ 18	0 ≤ <i>h</i> ≤ 15, 0 ≤ <i>k</i> ≤ 15, –19 ≤ <i>l</i> ≤ 0
Scan mode	Φ 0–170°, ΔΦ = 1.5°	ω
Program data collection	Stoe Expose	Siemens P3
Program data reduction	Stoe Integrate	PROFIT (Strel'tsov and Zavodnik, <i>Kristallographia</i> 6 (1989) 1369)
Reflections collected	9379	2577
Reflections observed [<i>I</i> > 2σ(<i>I</i>)]	2161	2402
Independent reflections	2851 [<i>R</i> _{int} = 0.03]	2577
Reflections used	2851	2544
Absorption correction	Indexed faces	None
Maximum and minimum transmissions	0.9691, 0.8392	
Structure solutions	Direct methods	Direct methods
Structure refinement	Full matrix on <i>F</i> ²	Full matrix on <i>F</i> ²
Programs used	SHEXRTL-PLUS, SHELXS-97 (Sheldrick, 1997), SHELXL-97 (Sheldrick, 1997), Stoe IPDS software	SHEXRTL-PLUS, SHELXS-97 (Sheldrick, 1997), SHELXL-96 (Sheldrick, 1996)
Extinction coefficient		0.0303(14)
Weighting parameter	0.0482, 0	0.0544, 1.1804
Number of refined parameters	248	249
<i>R</i> (observed reflections)	0.0294	0.0344
<i>wR</i> ₂ (used reflections)	0.0750	0.0932
Goodness-of-fit on <i>F</i> ²	0.938	1.067
Largest difference peak and hole (e Å ⁻³)	0.273 and –0.327	0.256 and –0.378

difference Fourier synthesis and refined in the isotropic approximation. Crystallographic data are collected in Table 1.

3.4. Thermal isomerization of complex **2** monitored by ¹H-NMR in C₆F₆

To 15 mg of the complex **2** 0.6 ml of C₆F₆ was added until complete dissolution of the complex and the solution was then heated for different time intervals in sealed and carefully degassed 5 mm NMR tubes at

90 ± 0.5 °C in a thermostat. After respective time intervals, the sample tube was removed from the thermostat and rapidly cooled to ambient temperature. The ratio [3]/[2] was then measured by means of ¹H-NMR.

3.5. Synthesis of **3** via thermal isomerization of **2** in decane

Complex **2** (100 mg) was dissolved in 50 ml of degassed decane, the solution was then heated for different time intervals in sealed glass tubes at 100 ±

0.5 °C in a thermostat. After respective time intervals, the sample tubes were rapidly cooled to ambient temperature. The course of the rearrangement during the first stage was monitored by chromatography. After TLC in order to remove decane one-tenth of the solution volume was transferred to a small column (silica) and eluted with hexane. The mixture of the complexes was then eluted with benzene. Prolonged heating and removal of solvent yielded red crystals of **3**. ¹H-NMR (300 K, C₆D₆, 400.1 MHz, ppm): δ = 5.43 (2H, m, H1, H4), 4.65 (2H, m, H2, H3), 7.40 (2H, dt, J_{H8/H9} = 7.99 Hz, J_{H7/H9} = 0.84 Hz, H9, H11), 7.21 (2H, dd, J_{H7/H8} = 7.04 Hz, J_{H7/H4} = 0.8 Hz, H7, H13), 7.17 (2H, 't', H8, H12). ¹H-NMR (300 K, C₆F₆, 400.1 MHz, ppm): δ = 6.44 (2H; m, H1, H4), 5.75 (2H, m, H2, H3), 7.91 (2H, d, J_{H7/H8} = 8.30 Hz, J_{H7/H9} = 0.50 Hz, H9, H11), 7.95 (2H, d, J_{H7/H8} = 7.10 Hz, J_{H7/H4} = 0.62 Hz, H7, H13), 7.78 (2H, dd, H8, H12). ¹³C-NMR (300 K, C₆D₆, 100.6 MHz, ppm): δ = 97.58 (C2, C3), 90.07 (C1, C4), 106.22 (C5, C15), 119.98 (C7, C13), 127.37 (C9, C11), 128.29 (C8, C12), 135.03 (C16), 130.37 (C10), 233.64 (C0). Mass spectra: *m/e* 338 (3.8) [M⁺]; 282 (7.2) [M – 2CO]⁺; 254 (33.9) [M – 3CO]⁺; 202 (100) [C₁₆H₁₀⁺], 52 (62.1) [Cr⁺]. IR (cm⁻¹): ν_{CO} = 1920, 1988. C₁₉H₁₀O₃Cr: Calc.: C, 67.46; H, 2.96. Found: C, 67.01; H, 2.90%. Crystals suitable for X-ray diffraction were obtained by layering of solution of **3** (30 mg in 10 ml of benzene) with 35 ml of hexane at 5 °C for ca. 3 weeks.

3.6. X-ray structure analysis of **3**

Accurate cell parameters and orientation matrices were obtained by least-squares refinement of 24 carefully centered reflections in the 23° ≤ 2θ ≤ 27° range. Two standard reflections were monitored every 98 reflections for **3** and showed no significant variation. Data were corrected for Lorentz and polarization effects. The carefully chosen rather small, well-formed and essentially isometric single crystal, the quality of obtained results, and the relatively low values of the absorption coefficient justified neglect of an absorption correction. The structure was solved by direct methods and subsequent difference Fourier maps. All hydrogen atoms were located in the difference Fourier synthesis and refined in the isotropic approximation. Crystallographic data are collected in Table 1.

3.7. Attempted isomerization of complex **3**

Thermal treatment of **3** was performed analogously to that of **2**. Even after maintaining samples of **3** at

130 °C for 40 h both in the solution (decane, benzene, hexafluorobenzene) as well as in the molten form, spectral evidence for the process **3** → **2** was absent.

Acknowledgements

This work was supported by the Volkswagen Foundation (Grant I/71351).

References

- [1] (a) G. Wilkinson, F.G.A. Stone, E.W. Abel (Eds.), *Comprehensive Organometallic Chemistry*, vol. 5, Pergamon Press, London, 1994, p. 501; (b) Yu.F. Oprunenko, *Russ. Chem. Rev.* 69 (2000) 683.
- [2] Yu.F. Oprunenko, S.G. Malyugina, Yu.A. Ustynyuk, N.A. Ustynyuk, *Izv. Akad. Nauk SSSR Ser. Khim.* (1984) 2405 (*Chem. Abstr.* 102 (1985) 132198e).
- [3] E.P. Kündig, V. Desorby, C. Grivet, B. Rudolf, S. Spichiger, *Organometallics* 6 (1987) 1173.
- [4] Yu.F. Oprunenko, S.G. Malyugina, Yu.A. Ustynyuk, N.A. Ustynyuk, D.N. Kravtsov, *J. Organomet. Chem.* 338 (1988) 357.
- [5] S.D. Cunningham, K. Öfele, B.R. Willeford, *J. Am. Chem. Soc.* 105 (1983) 3724.
- [6] Yu.F. Oprunenko, I.A. Shaposhnikova, Yu.A. Ustynyuk, *Organomet. Chem. USSR* 4 (1991) 684 (and references therein).
- [7] Yu.F. Oprunenko, et al., *J. Organomet. Chem.* 583 (1999) 136 (special issue dedicated to Professor Alberto Cecon).
- [8] (a) R.U. Kirss, P.M. Treichel Jr., *J. Am. Chem. Soc.* 108 (1986) 853; (b) P. Berno, A. Cecon, F. Daprà, A. Gambaro, A. Venzo, *J. Chem. Soc. Chem. Commun.* (1986) 1518.
- [9] N.G. Akhmedov, S.G. Malyugina, V.I. Mstislavsky, Yu.F. Oprunenko, V.A. Roznyatovsky, Yu.A. Ustynyuk, *Organometallics* 17 (1998) 4607.
- [10] T.A. Albright, P. Hofmann, R. Hoffmann, P. Lillya, P.A. Dobbosh, *J. Am. Chem. Soc.* 105 (1983) 3396.
- [11] K. Nicholas, R. Kerber, E. Stiefel, *Inorg. Chem.* 10 (1971) 1519.
- [12] E.P. Kündig, C. Perret, S. Spichiger, G. Bernardinelli, *J. Organomet. Chem.* 286 (1985) 183.
- [13] C. White, S.J. Thompson, P.M. Maitlis, *J. Chem. Soc. Dalton Trans.* (1977) 1654.
- [14] Rapid solvolytic ligand displacement is, however, observed for the radical cation [(η⁶-naphthalene)₂chromium(I)]⁺. Ch. Elschenbroich, R. Möckel, W. Massa, M. Birkhahn, U. Zenneck, *Chem. Ber.* 115 (1982) 334.
- [15] R. Benn, R. Mynott, I. Topalovic, F. Scott, *Organometallics* 8 (1989) 2299.
- [16] A. Stanger, H. Weismann, *J. Organomet. Chem.* 515 (1996) 183.
- [17] Ch. Elschenbroich, R. Möckel, A. Vasil'kov, B. Metz, K. Harms, *Eur. J. Inorg. Chem.* (1998) 1391.
- [18] B. Deubzer, E.O. Fischer, H.P. Fritz, C.G. Kreiter, N. Kriebitzsch, H.D. Simmons Jr., B.R. Willeford, *Chem. Ber.* 100 (1967) 3084.
- [19] K. Öfele, *Chem. Ber.* 99 (1966) 1752.
- [20] (a) M.F. Bailey, L.F. Dahl, *Inorg. Chem.* 4 (1965) 1314; (b) B. Rees, P. Coopens, *Acta Crystallgr. Sect. B* 29 (1973) 2515.
- [21] V. Kunz, W. Nowacki, *Helv. Chim. Acta* 50 (1967) 1052.